https://doi.org/10.18524/1810-4215.2024.37.313643

ANGULAR BRIGHTNESS DISTRIBUTION OF QUASAR 3C268.4 AT DECAMETER WAVELENGTHS

R.V. Vashchishin[1], V.O. Shepelev[2], O.O. Litvinenko[3], A.B. Lozinsky[4]

[1] Gravimetric Observatory of the Institute of Geophysics of the NAS of Ukraine Poltava, Ukraine, *vrv.uran2@gmail.com*

[2] Institute of Radio Astronomy of the NAS of Ukraine, Kharkiv, Ukraine

[3] URAN-4 Observatory of the Institute of Radio Astronomy of the NAS of Ukraine, Odesa, Ukraine

[4] Karpenko Physico-Mechanical Institute of the NAS of Ukraine, Lviv, Ukraine

ABSTRACT. Using the URAN VLBI network, we studied an angular structure of the 3C268.4 quasar at the decameter wavelengths. It is shown, that the brightness distribution of the source in the decameter range differs significantly from the decimeter image of the quasar. At low frequencies, the source model consists of two extended components and a compact feature, whose sizes and positions coincide with the parameters of lobes and one of the hot spots of 3C268.4 observed in the decimeter range. The radio emission of the second hot spot at decameter wavelengths is quite weak and does not significantly affect interferometer response. The probable spectra of the quasar components and their changes in the range from decameter to decimeter wavelengths are determined in the study as well. It is noted that, in contrast to the high-frequency image, where compact hot spots predominate in the 3C268.4 radiation, at decameter wavelengths about 65% of the source flux density is provided by more extended lobes. We have also shown that the change in the slope of the full spectrum of the quasar at 230 MHz is caused by synchrotron losses in its lobes.

Keywords: decameter range, brightness distribution, decameter model.

АНОТАЦІЯ. За допомогою РНДБ мережі УРАН, було досліджено кутову структуру квазара 3C268.4 на декаметрових довжинах хвиль. Показано, що розподіл яскравості джерела в декаметровому діапазоні суттєво відрізняється від дециметрового зображення квазара. На низьких частотах модель джерела складається з двох протяжних компонентів і одного компактного елемента, розміри і положення яких збігаються з параметрами пелюсток і однієї з гарячих плям 3C268.4, що спостерігаються в дециметровому діапазоні. Радіовипромінювання другої гарячої плями на декаметрових довжинах хвиль досить слабке і не впливає істотно на відгук інтерферометра. У дослідженні також визначаються ймовірні спектри компонентів квазара та їх зміни в діапазоні від декаметрових до дециметрових довжин хвиль. Відзначається, що на відміну від високочастотного зображення, де в випромінюванні 3C268.4 переважають компактні гарячі плями, на декаметрових хвилях близько 65% густини потоку джерела забезпечується більш протяжними пелюстками. Ми також показали, що зміна нахилу повного спектру квазара на частоті 230 МГц викликана синхротронними втратами в його пелюстках.

Ключові слова: декаметровий діапазон; розподіл яскравості; декаметрова модель

1. Introduction

Studies of extragalactic radio sources associated with active galactic nuclei have shown that most such sources have a structure in the decameter range noticeably different from their images observed at shorter wavelengths. To investigate this difference, we observe radio galaxies and quasars with the URAN interferometers at the lowest frequencies.

The radio source 3C268.4 optically associated with a quasar at a redshift of 1.4 has an FRII-type structure at decimeter wavelengths (Reid et al., 1995). It consists of a weak core and two radio lobes with hot spots at their ends spaced 10" apart. The southwestern hot spot provides about 68% of the total source flux density while the northern-eastern one does only 10%. Their angular sizes are about 1". The rest of the radiation comes from the more extended lobes of the source. The lowest frequency where the 3C268.4 structure was earlier studied with MERLIN was 408 MHz (Lonsdale & Morrison, 1983). The total source spectrum is bent near the frequency 230 MHz (Herbig & Readhead, 1991) showing a possibility of structure modifications at lower frequencies. The source power and angular dimensions of its components are suitable for its observation with the URAN interferometers (Megn et al., 1997) in the decameter range and the study of this quasar was never conducted before at such low frequencies.

2. Observations and data reduction

Observations of 3C268.4 were carried out using the URAN interferometer network at 20 and 25 MHz simultaneously. Signals were recorded in separate 10-minute

scans at hour angles of +/-150 minutes relative to the culmination moment. Interferometer pairs were formed by multiplying the recorded signals of the north-south antenna of the UTR-2 radio telescope with the signals of each URAN antenna.

It is known that the visibilities obtained at different baselines carry information about the brightness distribution of the object under study. With good filling of the UV plane, the source brightness distribution can be reconstructed by the inverse Fourier transform of the set of their complex values. However, we do not use this approach with URAN due to the limited number of baselines and insufficient filling of the UV plane. Besides that visibility phases at decameter wavelengths are severely distorted by the influence of the propagation medium which makes it impossible to apply direct mapping methods. Therefore, to reconstruct radio images of sources in the decameter wavelength, we use the method of fitting the brightness distribution models only by the visibility modules.

The method is described in (Megn et al., 2001) and consists in representing the real brightness distribution at the map of the source by a model consisting of a certain number of elliptical components with Gaussian brightness distribution. Then changing the parameters of this initial model and calculating its interferometric response we use the least squares method to minimize the differences between calculation and experimental data collected with the URAN interferometers. The result of the fitting procedure is a model distribution of brightness at decameter wavelengths consistent with the URAN observational data.

We used the map obtained with the VLA at 1.69 GHz (the NVAS can be browsed through http://www.vla.nrao.edu/astro/nvas/) to determine the initial model for fitting the low-frequency model of 3C268.4. The parameters of the initial model are given in Table 1.

Table 1: The model of brightness distribution of 3C268.4 fitted to a 1.69 GHz map

	α,"	δ,"	S/S_0,%	θ,"	a/b	ψ,°
HS_{NE}	3.5	3.2	10	0.9	1	0
L_{NE}	3.5	3.2	6	1.9	1.2	90
Core	0	0	1	0.9	1	0
HS_{SW}	–2.1	–3.7	68	1.1	1.7	128
L_{SW}	–2.1	–3.6	15	2.1	1.4	128

Notes:
HS – hot spot; *L* – lobe;
α, δ – coordinates of the components center;
θ – size at a half power level;
a/b – ellipticity;
ψ – position angle of the component;
S/S_0 – percentage of total flux.

As an example, measured with the URAN-2 and URAN-3 interferometers the experimental dependences of the visibility modules on hour angle are shown in Fig. 1 and Fig. 2 by symbols *3*. Line *1* marks the response of the initial high-frequency model at these baselines, and shows what visibilities measured at decameter band would be if the image of the radio source did not change with frequency decreasing. A noticeable distinction between this

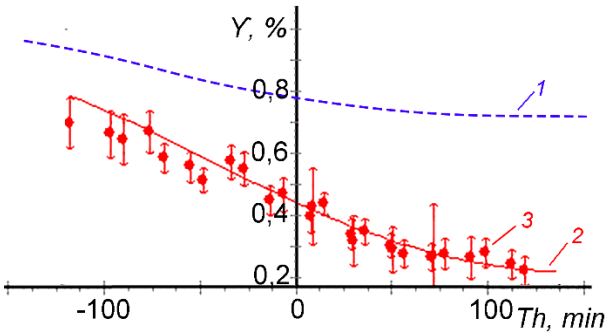

Figure 1: Visibility module of the decameter model for the URAN-2 interferometer: *1* – high frequency model; *2* – fitted decameter model; *3* – experimental data

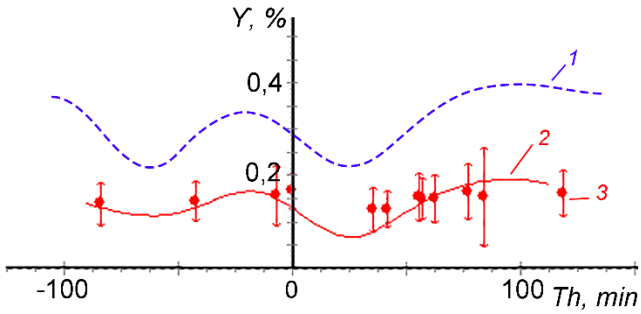

Figure 2: Visibility module of the decameter model for the URAN-3 interferometer at 25 MHz: *1* – high-frequency model; *2* – fitted decameter model; *3* – experimental data

curve from experimental data means changes in the source structure. A low-frequency model was then fitted based on experimental data obtained with all interferometers of the URAN network at frequencies of 20 and 25 MHz. The calculated responses of the fitted model at 25 MHz for URAN-2 and URAN-3 are shown in Fig. 1 and Fig. 2 by line *2*.

The parameters of the decameter model at frequencies of 20 and 25 MHz are given in Table 2.

Table 2. The decameter model at frequencies at 20 and 25 MHz

	α,"	δ,"	S/S_0,%	θ''_{25}	θ''_{20}	a/b	ψ,°
HS_{NE}	3.5	3.2	9	1.1	1.3	1	0
L_{NE}	3.5	3.2	32	2.8	3.1	1	0
HS_{SW}	–2.1	–3.7	26	1.1	1.2	1.7	128
Lsw	–2.1	–3.6	33	4.1	4.3	1.4	128

3. The results

By comparing the two tables, it is easy to see what is causing the discrepancies observed. At high frequencies, the main contribution to the total flux density is made by compact details – hot spots. Their fraction in the total flux of the quasar is about 78%, while at low frequencies the total source radiation is predominantly formed by extended details – lobes. Their contribution to the source total flux in the decameter range is about 65%. Fig. 3 and Fig. 4 show the high-frequency and decameter models on a loga-

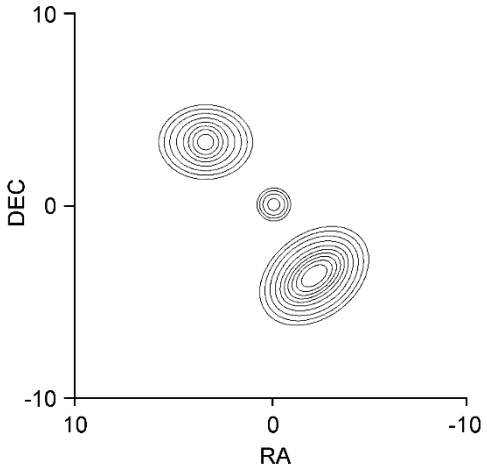

Figure 3: Model fitted to 1.69 GHz map

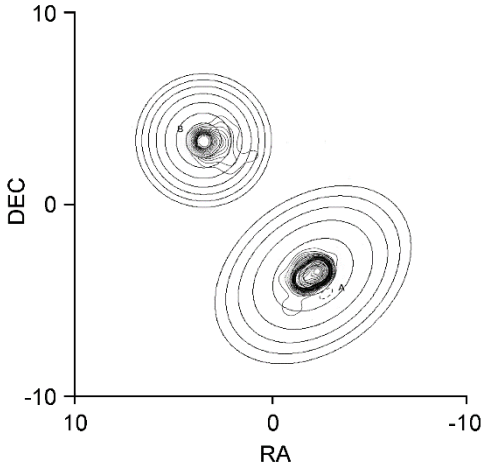

Figure 4: Decameter model overlaid on a 408 MHz map

rithmic scale of brightness. The latter model is shown against the background of a 408 MHz map with an angular resolution of 0.9" (Lonsdale & Morrison, 1983).

Fig. 5 shows the total spectrum of the quasar – *1* and probable spectra of its components: *2* and *4* – spectra of the southwestern and northeastern hot spots, *3* and *5* – southwestern and northeastern lobes. The spectral index of each spectrum is shown in the same color above it.

Linear approximation of the total spectrum was performed by the least squares method separately for the sections from 20 to 230 MHz and above 230 MHz according to the data of (Kellermann & Paulini-Toth, 1969; Viner & Erickson, 1975; Laing & Peacock, 1980; Roger et al., 1986). Spectra of hot spots – according to our data, obtained at frequencies of 20 and 25 MHz and data at 1.69 and 4.8 GHz.

As can be seen from the figure, a bend is observed in the total spectrum at a frequency of about 230 MHz. This bend is related to the behavior of the lobe spectra, typical for synchrotron losses. The lobe spectra in this figure were obtained by subtracting the hot spot spectra from the total spectrum, taking into account the ratio of lobe fluxes at 20, 25 MHz, and 1.69 GHz.

Knowing the magnetic field strength in the lobe (Liu et al., 1992) and the inflection point of the spectrum, using formula (1) from (Liu et al., 1992), we can calculate the synchrotron age of the quasar, i.e. the time that has passed

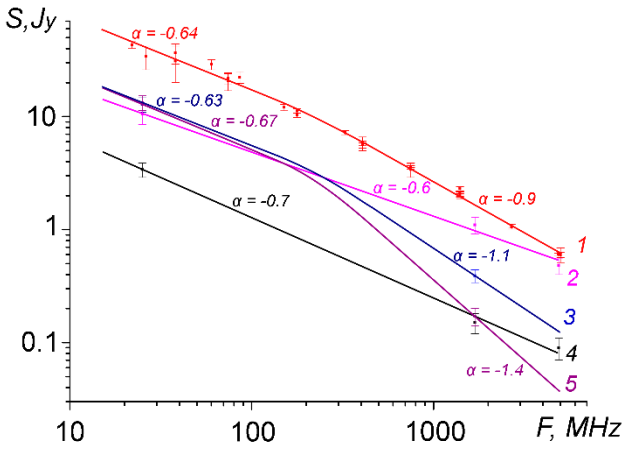

Figure 5: The total spectrum of 3C268.4 and the probable spectra of its components: *1* – total spectra; *2* – southwestern hot spot; *3* – southwestern lobe; *4* – northeastern hot spot; *5* – northeastern lobe

since the last acceleration of electrons. According to our data, the age of the quasar is about 8.4 million years.

It should be noted here, that the ratio of the fluxes of the source components, calculated by us at a frequency of 408 MHz, agrees well with the data of (Lonsdale & Morrison, 1983).

4. Conclusion

For the first time, an investigation of the angular structure of the quasar 3C268.4 was carried out in the decameter range. The most optimal model of the angular brightness distribution at frequencies of 20 and 25 MHz was obtained. It was found that:

1. The sizes of the source components increased compared to high-frequency ones due to interstellar scattering (in hot spots) and synchrotron losses (in lobes).

2. The main contribution to the total source flux at low frequencies is made by the lobes – 65% and the southern hot spot – 26%, which significantly differs from the high frequencies where nearly 78% of the total flux is provided by hot spots. The radio emission of the northern hot spot at decameter wavelengths is quite weak and does not significantly affect interferometer response.

3. It has been established that the bending of spectra at a frequency of about 230 MHz is caused by synchrotron losses. The approximate age of the source was found to be about 8.4 million years.

References

Herbig T., Readhead A.C.S.: 1992, *ApJS*, **81**, 83.
Kellermann K. I., Paulini-Toth I. I. K.: 1969, *ApJ*, **157**, 1.
Laing R.A., Peacock J.A.: 1980, *MNRAS*, **190**, 903.
Liu R., Pooley G., Riley J.M.: 1992, *MNRAS*, **257**, 545.
Lonsdale C.J., Morison I.: 1983, *MNRAS*, **203**, 833.
Megn A.V., Braude S.Ya., Rashkovsky S.L., et al.: 1997, *AJ*, **2**, 4, 385.
Megn A.V., Rashkovsky S.L., Shepelev V.A.: 2001, *RPRA*, **6**, 1, 9.
Reid A., Shone D.L., Akujor C.E. et al.: 1995, *A&AS*, **110**, 213.
Roger R.S., Costain C.H., Stewart D.I.: 1986, *A&AS*, **65**, 485.
Viner M.R., Erickson W.C.: 1975, *AJ*, **80**, 11, 931.